PAPER

Check for updates

Handheld device quantifies breath acetone for real-life metabolic health monitoring†

Grégoire M. G. B. H. Bastide,‡[ab] Anna L. Remund,‡[ab] Dina N. Oosthuizen, [iD][ac] Nina Derron, [iD][b] Philipp A. Gerber[b] and Ines C. Weber [iD] *[ab]

Non-invasive breath analysis with mobile health devices bears tremendous potential to guide therapeutic treatment and personalize lifestyle changes. Of particular interest is the breath volatile acetone, a biomarker for fat burning, that could help in understanding and treating metabolic diseases. Here, we report a hand-held (6 × 10 × 19.5 cm^3), light-weight (490 g), and simple device for rapid acetone detection in breath. It comprises a tailor-made end-tidal breath sampling unit, connected to a sensor and a pump for on-demand breath sampling, all operated using a Raspberry Pi microcontroller connected with a HDMI touchscreen. Accurate acetone detection is enabled by introducing a catalytic filter and a separation column, which remove and separate undesired interferents from acetone upstream of the sensor. This way, acetone is detected selectively even in complex gas mixtures containing highly concentrated interferents. This device accurately tracks breath acetone concentrations in the exhaled breath of five volunteers during a ketogenic diet, being as high as 26.3 ppm. Most importantly, it can differentiate small acetone changes during a baseline visit as well as before and after an exercise stimulus, being as low as 0.5 ppm. It is stable for at least four months (122 days), and features excellent bias and precision of 0.03 and 0.6 ppm at concentrations below 5 ppm, as validated by proton-transfer-reaction time-of-flight mass spectrometry (PTR-ToF-MS). Hence, this detector is highly promising for simple-in-use, non-invasive, and routine monitoring of acetone to guide therapeutic treatment and track lifestyle changes.

[a] Particle Technology Laboratory, Department of Mechanical and Process Engineering, ETH Zurich, CH-8092 Zurich, Switzerland. E-mail: iweber@ethz.ch
[b] Department of Endocrinology, Diabetology, and Clinical Nutrition, University Hospital Zurich (USZ) and University of Zurich (UZH), CH-8091 Zurich, Switzerland
[c] Department of Mechanical and Industrial Engineering, Northeastern University, 467 Egan Center, 02115 MABoston, USA
† Electronic supplementary information (ESI) available. See DOI: https://doi.org/10.1039/d3sd00079f
‡ Shared first author.

1. Introduction

Mobile health (mHealth) devices[1] could enable new strategies toward predictive, personalized, participatory, and preventative (4P) medicine.[2] Particularly promising is breath analysis due to its easy accessibility and non-invasive application.[3] From routine detection of biomarkers in exhaled breath, abnormal patterns could be recognized at an early stage for screening of diseases. Furthermore, longitudinal monitoring could be applied to provide user feedback at the point-of-care[4] and facilitate personalized treatment and prevention.

Metabolic diseases, including obesity and diabetes, are major health concerns that pose a significant threat to public health, with growing prevalence every year.[5] In total, 13% of the world's adult population and 39 million children under the age of 5 were obese in 2016 and 2020, respectively, while diabetes accounted for 1.5 million deaths in 2019.[6] In general, obesity is a preventable disease,[7] but weight loss is highly complex and individual, and a lack of motivation to maintain lifestyle changes is one of the many major problems. Hence, monitoring metabolic processes on a personalized level with mHealth devices is of tremendous interest to guide dieting and exercise and could have significant implications for the management and treatment of metabolic diseases.

A promising breath biomarker is acetone that evolves from the metabolization of fatty acids and reflects the state of lipolysis.[8] Basal acetone concentrations after overnight fasting are typically around 1 part per million (ppm),[9] but increase during physical exercise or dieting. Specifically, acetone levels increased during exercise (*e.g.*, by 12% in high-fit individuals[10] or 25% during graded exercise[11]) and showed a two-fold increase three hours after an exhaustive[10] or moderate[12] exercise stimulus. An increase in exhaled acetone or blood ketone bodies is also observed during intermittent fasting (*e.g.*, by 35% during alternate day fasting[13]), and may go beyond 20 ppm during a ketogenic

diet.[14] It is worth noting that ketogenic diets are helpful in limiting seizures in epilepsy.[15] Moreover, elevated ketone levels have been correlated with beneficial health effects in mice, such as long-term health span improvements and cardioprotective effects.[16]

Chemical sensors[17] are promising to measure breath acetone due to their low power consumption,[18] high miniaturization potential,[19] and simplicity. A myriad of acetone sensing materials are available, for example, based on ZnO (*e.g.*, with Ni,[20] Al,[21] or $ZnFe_2O_4$ (ref. 22)), WO_3 (ref. 23) (*e.g.*, with TiO_2,[24] Cr,[25] or Si, as γ-,[26] or h-phase,[27] or with Pt-decorated nanotubes[28]), CuO (*e.g.*, with Ce,[29] or Cr (ref. 30)), or as composites (*e.g.*, SnO_2 with reduced graphene oxide,[31] with multi-walled carbon nanotubes,[32] with Ni–graphene[33]), to name a few. Still, these sensors often lack selectivity. This is due to the highly complex gas matrix of breath, containing more than 1000 volatiles[34] that can occur at concentrations orders of magnitude higher than acetone (*e.g.*, 10 ppm hydrogen[35]). Similarly, commercial devices for acetone detection (*e.g.*, LEVL, Ketonix, Keyto, Lexico Health Keto Breath Analyzer, ACE KETOSCAN mini) usually fall short on accuracy,[36] and are not established for routine healthcare monitoring.[37] Needed are acetone monitors that are handheld and low-power for on-demand use, feature long-term stability and plug-and-play characteristics for longitudinal monitoring, are easy-to-use, and feature a sufficient dynamic range (*i.e.*, between 0.5 and 20 ppm acetone) and precision (*e.g.*, to recognize fine exercise-induced changes) for 4P medicine.

Here, we present a stand-alone hand-held device for high-precision acetone monitoring in breath. Selectivity is achieved by introducing a previously developed room-temperature catalytic filter[38] and separation column[39] ahead of the sensor (Fig. 1a). The catalytic filter[40] serves by removing most of the critical breath interferents (*e.g.*, methanol, ethanol, and isoprene) through conversion to sensor-inert species (*e.g.*, CO_2), while the separation column retains the acetone longer than non-converted interferents (*e.g.*, hydrogen), which, consequently, reach the sensor sequentially. This way, the sensitive but non-specific chemo-resistive sensor quantifies acetone even at low ppb concentrations. The acetone sensitivity and selectivity are first characterized with synthetic gas mixtures containing breath-relevant volatiles (*e.g.*, acetone, methanol, ethanol, hydrogen, isoprene). Then, the device stability and dynamic range is assessed. This is followed by breath measurements with five volunteers during a ketogenic diet, during a regular work day (baseline visit), and before and after exercise.

2. Experimental

2.1 Device components, fabrication, and assembly

The stand-alone acetone device is shown in Fig. 1b, which comprises a sampling unit, a catalytic filter and separation column, a sensor, a Raspberry Pi coupled to a breadboard, and a pump, all protected by a casing. During operation,
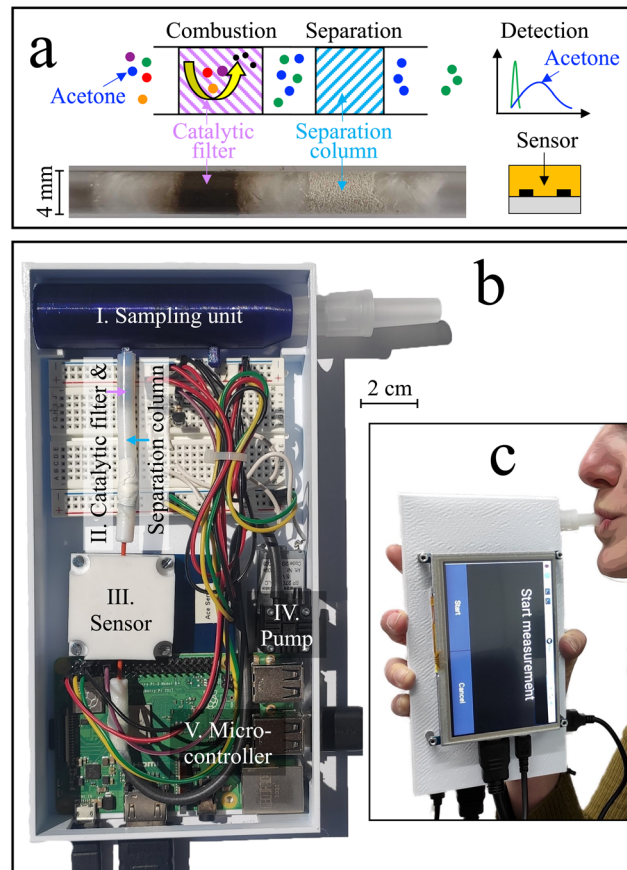

Fig. 1 (a) Detection concept. The catalytic filter removes undesired interferents by combustion to inert species. The remaining interferents are separated from acetone by the separation column, resulting in sequential, and hence selective detection. A photo of the catalytic filter and separation column contained inside a glass tube is provided for better visibility. (b) The device comprises an end-tidal breath sampling unit (I) that holds a sterile and disposable mouthpiece, a catalytic filter and a separation column contained in a Teflon tube (II) that combust and separate interferents from acetone, a chemo-resistive sensor enclosed in a Teflon chamber (III), a pump (IV) to provide a flow from the breath sampler to the sensor, and a Raspberry Pi microcontroller (V) connected to a breadboard for device operation, data collection, and data read-out. An external HDMI-touchscreen is fixed to the outside of the device casing as a control display. (c) Handheld breath acetone device during a measurement.

exhaled air was guided through the sampling unit (blue) holding a disposable and sterile mouthpiece (EnviteC-Wismar GmbH, Germany) to a catalytic filter and separation column contained in a Teflon tube, and finally to a sensor sitting inside a Teflon chamber. A pump (SP 270 EC-LC 5 V DC, Schwarzer Precision, Germany) was used for non-continuous breath sampling. All components were connected through inert Teflon tubing. A microcontroller (Raspberry Pi 3B+, Pi Shop, Switzerland) connected to a breadboard was used to control the sensor and pump, extract the data, and display them on the external touchscreen with a HDMI port (5 inch HDMI LCD (B), BerryBase, Switzerland). The Raspberry Pi was powered through its micro-USB port using a

power adapter or a power bank (Verico Power Guard XL, 10 000 mA h, Galaxus, Switzerland).

The breath sampling unit was designed with the Computer Aided Design (CAD) software NX12. A 3D printer (Original Prusa i3 MK3, Czech Republic) with a printing precision of 0.1 mm was used to fabricate the sampling units out of polyethylene terephthalate glycol (PETG). The detector was defined as the combination of the catalytic filter, the separation column, and the sensor. The catalytic filter was a packed bed made of 15 mg of 3 mol% Pt/Al_2O_3 nanoparticles fabricated by flame spray pyrolysis (FSP) and annealed at 700 °C for one hour, as described in detail elsewhere.[41] The separation column comprised 20 mg of Tenax TA (poly(2,6-diphenyl-p-phenylene oxide), 80–100 mesh, $\sim$35 $m^2 g^{-1}$, Merck, Switzerland). Both the Pt/Al_2O_3 nanoparticles and the Tenax TA powder were embedded between a layer of quartz sand and quartz wool inside a Teflon tube with 4 mm inner diameter. The commercial sensor (Adafruit SGP40, Sensirion AG, Switzerland) was enclosed in a Teflon-chamber and connected to the Raspberry Pi through the intended SDA, SCL, ground, and 3.3 V ports.

2.2 Laboratory sensing tests

The acetone device was tested with synthetic gas mixtures prior to the breath measurements. For this, the breath sampling unit and pump were removed. Then, the device (now at the catalytic filter) was directly connected to a gas measuring setup[42] through inert Teflon tubing. The setup provided a continuous flow of humidified (50% relative humidity, RH, unless mentioned otherwise) synthetic air (C_nH_m and $NO_x \leq 100$ ppb, Pan Gas, Switzerland) to the device using mass flow controllers (MFCs, Bronkhorst, Netherlands). Humidification was achieved by bubbling synthetic air through ultrapure water (Milli-Q A10, Merck, Switzerland) contained in a glass bubbler (Drechsel bottle, sintered glass frit, Merck, Switzerland), and validated by a humidity sensor (SHT2x, Sensirion AG, Switzerland). The overall flow rate was adjusted to 60 mL min^{-1}. Then, the setup dosed the calibration standards acetone (15 ppm), methanol (16 ppm), hydrogen (50 ppm), ethanol (15 ppm), and isoprene (17 ppm), all in synthetic air with C_nH_m and $NO_x \leq 100$ ppb (Pan Gas, Switzerland), into the humidified synthetic air stream. The sensor was evaluated both for single analytes and gas mixtures by applying analyte exposures of 30 s (unless mentioned otherwise). Note that the sensing tests were performed with the sensor alone, with the catalytic filter, and with both the catalytic filter and the separation column.

2.3 Device operation, calibration, and breath measurements

The acetone device was operated in a non-continuous mode, where the pump was running only during breath sampling, analysis, and recovery. Exhaled breath was collected with sterile, disposable mouthpieces, which were inserted into the breath sampling unit prior to the exhalation. Then, volunteers were instructed through the external HDMI-display to exhale into the device for 20 s. A visual countdown on the external HDMI display indicated when the 20 s were finished, and the breath exhalation stopped. The exact device operation procedure is described in the ESI.† The pump was turned on 5 s after the start of the breath exhalation, to ensure end-tidal[43] breath sampling (as verified by a commercial CO_2 sensor, Capnostat 5, Respironics, United States). The pump provided a constant gas flow of 60 mL min^{-1} for 700 s, as validated by a flow meter at its outlet. This way, first breath and then room air was drawn from the sampling unit through the catalytic filter, separation column, and to the sensor.

Device calibration was performed using liquid acetone calibration standards (10 mL in a 25 mL glass vial) that were prepared by diluting acetone (>95%, Merck, Switzerland) with defined volumes of ultrapure water (Milli-Q A10, Merck, Switzerland). The acetone headspace concentrations were determined with PTR-ToF-MS. Liquid rather than gas calibration standards were used due to their compactness and ease-of-use, which allows the hand-held device to be calibrated wherever needed. For calibration, the device breath sampling unit was removed, and a hypodermic needle (Sterican 0.9 × 70 mm, B. Braun, Switzerland) was connected instead through inert Teflon tubing. To perform the calibration, the headspace of the liquid standard was sampled by inserting the needle into the vial and sampling for 22 s (corresponding to 20 s of breath exhalation + 2 s that would be necessary to empty the breath sampling unit in case of a breath measurement). Afterwards, the needle was removed from the vial and room air was sampled to carry the headspace sample through the catalytic filter and separation column to the sensor. A second needle was inserted into the liquid of the vial to compensate for the pressure in the vial.

2.4 Study design

The breath study was carried out with five volunteers (four female) aged 24–33. All volunteers were free of known cardiovascular, respiratory, or metabolic diseases, non-smoking, and did not follow a specific diet (*e.g.*, low carb). During the breath study, the volunteers were asked not to drink (except water) or eat. The study comprised three separate visits: a baseline visit, an exercise visit, and a ketogenic diet visit. This study was approved by the responsible authority (ETH Zurich Ethikkommission, EK 2023-N-19), and each subject gave written informed consent prior to the tests.

Each visit started with a breath exhalation at 8:00 after overnight fasting of 11 h. During the baseline visit, volunteers provided hourly breath pulses until 12:00 (anthropometric data in Table S1†). During the exercise visit, the volunteers conducted a moderate exercise protocol (45

min cycling on an ergometer) at 63% (ref. 44) of the maximum heart rate (Table S1†) between 8:00 and 9:00, while maintaining a cadence of 70 rpm. The maximum heart rate was approximated for men by $HR_{max} = 223 - 0.9x$ and for women by $HR_{max} = 226 - x$, with x representing the participant's age (in years). The volunteers were asked to manually adjust the workload on the ergometer to maintain the desired heart rate. Thereafter, the volunteers provided hourly breath exhalations until 12:00. Note that volunteer #2 did not participate in the exercise appointment due to an injury.

The ketogenic diet visit took place on two subsequent days. On the first day, ketogenic meals were consumed at 9:00, 12:00 and 19:30. Participants provided breath exhalations at the following timestamps: 8:00, 9:30, 11:00, 12:30, 14:00, 15:30, and 17:00, and the following day at 8:00, 9:30, and 11:00. At 12:00 on the second day, they consumed a carbohydrate-rich lunch (i.e., pasta + tomato sauce) and their breath was analyzed again at 13:30 and 15:00. Note that on the second day, a longer measurement break was taken after consumption of the carbohydrate-rich lunch, since the body requires some time to switch from the lipid metabolism to the glucose metabolism.[45] The ketogenic meals were made by combining vegan Rama whipped cream 31% (Coop, Switzerland) with vanilla-flavored protein powder (Whey Protein 94, Switzerland) to reach a ratio of fat : (carbohydrate + protein) 4 : 1 KD based on the Johns Hopkins protocol.[46] The total amount of three ketogenic meals corresponded to 75% of the daily energy expenditure, which was determined by multiplying the resting energy expenditure (REE) of each volunteer with a physical activity factor, as described in detail in previous studies (Table S1†).[14] The REE was calculated using the revised Harris–Benedict formula.[47] The physical activity factor was based on the physical activity during working and leisure time, being 1.6 for the participating volunteers.

2.5 Validation with mass spectrometry

Breath measurements were analyzed simultaneously with a PTR-ToF-MS 1000 (Ionicon) connected at the pump outlet of the device. The PTR-ToF-MS was operated at a drift voltage of 600 V, a temperature of 60 °C, and a pressure of 2.3 mbar using H_3O^+ ions as the primary ion source. Analyte concentrations were determined at mass-to-charge (m/z) ratios of 47.05 (ethanol[48]), 59.05 (acetone[49]), 61.05 (isopropanol[50]), and 69.07 (isoprene[51]). For quantification, the PTR-ToF-MS was five-point calibrated with the catalytic filter and the separation column (for acetone) or only the separation column (for the remaining analytes) over the relevant range prior to the study using the above calibration gas standards. Breath acetone concentrations measured by the PTR-ToF-MS were quantified at the maximum acetone signal intensity detected during the breath exhalation.

2.6 Data analysis

The sensor response (S) was calculated as:

$$S = \frac{R_{air}}{R_{analyte}} - 1$$

with R_{air} and $R_{analyte}$ being the sensing film resistances in air and during analyte exposure, respectively. As per the IUPAC guidelines,[52] the selectivity of the sensor was determined by comparing the response of acetone to that of the interferents. The signal-to-noise ratio (SNR) was determined by dividing the response by the standard deviation of the baseline, measured over a minimum of 20 data points. The retention time (t_r) was calculated as the time elapsed between the start of exposure and the maximum response.[53] For breath measurements, the acetone response was evaluated at a retention time of 125 s. Acetone quantification was done by comparing this acetone response to liquid calibration standards.

For experimental measurements that were repeated at least three times, the average value ± standard deviation (σ) was calculated. The sample size (N) was indicated in the figure legends for each statistical analysis. The coefficient of determination (R^2) and Pearson coefficient (r_p) were calculated to assess the agreement and linearity between the acetone device and the PTR-ToF-MS and compare to the pertinent literature. The power-law functions were determined using Microsoft Excel (version 16.73). Bland–Altman analysis[54] was performed to compare the device data to the PTR-ToF-MS and quantify the device bias and precision. Therein, the bias[55] (i.e., estimate of a systematic measurement error) corresponded to the average difference between the device and PTR-ToF-MS. The precision was defined as $1.95 \times \sigma$, with σ being the standard deviation, due to the large number of samples (i.e., ≥ 38).[56] The bias and precision were evaluated for the lower concentration range (i.e., smaller than 5 ppm). For the full range of concentrations, the data was subjected to a square root transformation, resulting in a normal distribution of the differences (Shapiro–Wilk normality test with $p = 0.53$).[57] Square root transformation was chosen over logarithmic and reciprocal transformations as it best satisfied the requirement of normal variance. The mean difference and limits of agreement (with 95% confidence intervals) were calculated based on the transformed data and then back-transformed at the end.

3. Results and discussion

3.1 Principle of selective acetone detection

Fig. 1c shows the handheld device in operation, with dimensions of $6 \times 10 \times 19.5 \text{ cm}^3$ and a weight of 490 g. Simple device operation is enabled through the attached touch-screen, and continuous operation for at least 7 h is possible with a standard power bank, owing to the rather low power consumption (~3.75 W). Before evaluating the device
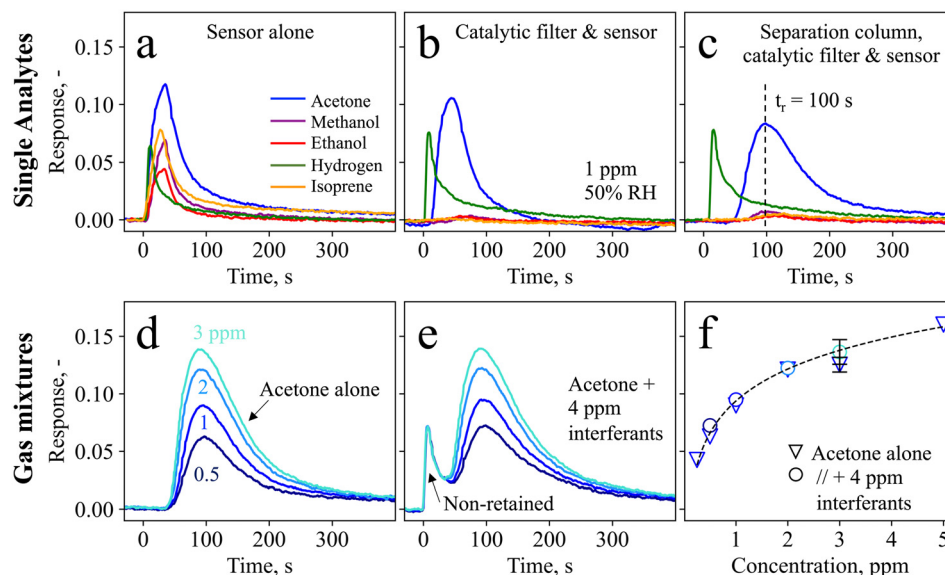
Fig. 2 Sensor response to 30 s exposure to 1 ppm acetone (blue), methanol (purple), ethanol (red), hydrogen (green), and isoprene (orange) (a) with the sensor alone, (b) with the sensor pre-screened by the catalytic filter, and (c) with the sensor pre-screened by both the catalytic filter and the separation column. The catalytic filter continuously removes interferents such as methanol, ethanol, and isoprene to sensor–inert species (e.g., CO_2), while the separation column retains the acetone, leading to sequential and thus selective detection of first hydrogen and then acetone. The acetone retention time (t_r) is indicated in (c) with a dashed line. Detector (i.e., catalytic filter + separation column + sensor) response to 0.5–3 ppm acetone as a single analyte (d) and in a gas mixture with additional methanol, ethanol, hydrogen, and isoprene, 1 ppm each (e). Note that higher acetone concentrations were not investigated due to a limitation of the measurement setup. (f) Respective calibration curve as a function of concentration for acetone as a single analyte (triangles, with additional 0.25 and 5 ppm concentrations) and in a gas mixture (circles). The error bar represents three different detectors. All measurements were performed in synthetic air at 50% RH.

in real breath, it is tested with laboratory gas mixtures containing the target analyte acetone as well as critical breath interferents. Specifically, ethanol, methanol, hydrogen, and isoprene are chosen as interferents, as they may occur at elevated concentrations in breath (e.g., >1.5 ppm methanol,[58] >0.6 ppm isoprene,[59] and >10 ppm hydrogen[35]) or surrounding air (e.g., >100 ppm ethanol from hand disinfectants[60]).

Fig. 2a shows the response of the sensor alone when exposed to 1 ppm of acetone, methanol, ethanol, hydrogen, and isoprene for 30 s. The sensor responds to each gas immediately, featuring similar responses for acetone (i.e., 0.12), isoprene (0.08), methanol (0.07), hydrogen (0.06), and ethanol (0.04), as expected for such non-specific chemo-resistive sensors. When pre-screening the sensor with the catalytic room-temperature[41] Pt/Al_2O_3 filter, the response towards ethanol, methanol, and isoprene is mostly removed (response < 0.004, Fig. 2b). In fact, flame-made Pt/Al_2O_3 catalysts have been reported to convert these interferents even at concentrations of up to 100 ppm,[41] owing to the high reactivity of well-dispersed Pt clusters and a preferential conversion of alcohols over acetone on Al_2O_3.[61] At the same time, acetone is hardly affected by the catalytic filter (response of 0.11), while a slight retention, probably due to sorption effects, is visible. Unfortunately, the catalytic filter cannot remove hydrogen, in line with the literature.[41]

Hence, acetone selectivity towards hydrogen is enabled by a separation column that retains acetone and delays it

by 100 s (Fig. 2c). Meanwhile, hydrogen passes the column unhindered and with a comparable response of 0.075. This leads to a timely separation between these two molecules, where almost no overlap is observed at the maximum acetone response, resulting in its selective detection. Note that the acetone retention results in a response reduction from 0.11 to 0.075, which is however still sufficient for the targeted application. Full detector recovery back to the baseline is obtained after ten minutes. Notably, the separation column alone (i.e., without the catalytic filter) is not sufficient to separate acetone from the interferents (Fig. S1†). The retention of acetone is due to the Tenax particles, which separate molecules mainly through unspecific adsorption via Van der Waals forces. This causes heavier molecules, such as acetone (with a molecular weight of 58 g mol^{-1}), to be retained for a longer time and to have higher breakthrough volumes[62] than interfering molecules like hydrogen (2 g mol^{-1}). The retention characteristics can be altered by adjusting the gas flow rate and exposure times (Fig. S2†), as well as the separation column loading, as has been explored for the detection of methanol (in breath[39] and hand sanitizers[63] as integrated device[64]) and formaldehyde.[65]

To assess the detector performance in gas mixtures containing acetone together with higher concentrated interferents, it is exposed to 0.5–3 ppm acetone alone (Fig. 2d) and in gas mixtures with each 1 ppm of methanol, ethanol, hydrogen, and isoprene (Fig. 2e). Without

interferents, the detector measures each acetone concentration at an almost identical retention time (100 ± 3 s), and clearly differentiates even between 0.5 and 1 ppm. Most importantly, when exposed to the gas mixtures, the acetone response hardly changes. This confirms again that the interferents are either catalytically removed (*i.e.*, in the case of ethanol, isoprene, and methanol, as shown in Fig. 2b), or separated from acetone (*i.e.*, in the case of hydrogen through the separation column, Fig. 2c). In fact, the first peak at $t = 0$ s with a response of 0.07 is in good agreement with the hydrogen response in Fig. 2c (response = 0.075). Notably, this detector is promising also for the detection of hydrogen, as is shown in Fig. S3† for 1–5 ppm hydrogen, which may be interesting for example to test for lactose intolerance[66] or for early diagnosis of necrotizing enterocolitis.[67]

The acetone responses as single analytes and in gas mixtures are shown in Fig. 2f, showing also the detector response to 0.25 (SNR = 50) and 5 ppm acetone. The measurements for single analytes and gas mixtures are in good agreement (<15% deviation), as is reproducibly shown for three separate detectors (*i.e.*, three different catalytic filters, separation columns, and sensors) represented by the error bar. A power-law response behavior is observed, typical for such chemo-resistive sensors in agreement with non-linear diffusion–reaction theory.[68] In addition, the detector exhibits high robustness also to 10–90% RH when tested with a gas mixture containing acetone and hydrogen, resulting in an acetone response of 0.08 ± 0.006 (Fig. S4†). This is beneficial for practical applications such as breath analysis, where the humidity in indoor and outdoor air (*e.g.*, 32–84% RH[69]) varies significantly and reaches >90% in breath.[70]

Fig. 3 Device response to liquid calibration standards (sampled in the headspace of the glass vial through a needle) over 122 days. Mean response and standard deviation are indicated. The error bar represents the standard deviation of three identically prepared detectors (*i.e.*, three different catalytic filters, separation columns, and sensors). The inset shows the device response to calibration standards containing 0.6–21.6 ppm acetone. Note that the device responses in room air differ from the flow-bench measurements (Fig. 2), likely due to differences in the flow conditions and baseline resistance.

3.2 Device stability, plug-and-play, and dynamic range

To move from the laboratory bench to point-of-care monitoring, breath devices and consumables need to be compact, low-cost, and easily replaceable. This includes calibration standards, which are frequently used to ensure precision and accuracy of commercial chemical devices (*e.g.*, LEVL). Therefore, device calibration and stability tests were carried out with liquid calibration standards comprising readily available and low-cost chemicals (*i.e.*, water and acetone) that can be prepared by simple dilution series.

Of crucial importance is device stability, as this determines whether it can be used for longitudinal monitoring, and how often device calibrations need to be performed. Fig. 3 shows the device response when sampling the headspace of the calibration standard containing 2.9 ppm of acetone over four months (122 days). Most importantly, no device deterioration is observed over the entire time, as demonstrated by the fairly constant response of 0.075 ± 0.002. In addition, daily variances are rather small (*i.e.*, ± 3%), outperforming other acetone detectors that showed larger variances (*i.e.*, 23% (ref. 71)) and required daily calibrations, or did not determine stability.[72] This signifies that this device, after initial calibration, does not require further calibrations within at least four months of operation, a big benefit for individual users who want to perform longitudinal measurements (*e.g.*, for personalized and participatory point-of-care medicine) with minimal time and effort. Beyond the four months of operation tested here, the calibration could be used also as an indicator of separation column or catalytic filter degradation and need for replacement.

Notably, exchanging the device detector components (*i.e.*, sensor, catalytic filter, and separation column) yields comparable results for three independent systems (error bar at 0 days, Fig. 3, showing deviations <15%), highlighting the potential for plug-and-play, where modular device units can be flexibly exchanged on-demand. The device dynamic range is displayed in the inset of Fig. 3, showing its response to 0.6–21.6 ppm acetone. The response follows a power-law function, in line with Fig. 2f, and the device is capable of differentiating small acetone concentrations that are relevant for fasting[13] and exercise applications (*e.g.*, <5 ppm[71]), as well as higher acetone concentrations that may be found during ketogenic diet (*e.g.*, >20 ppm[14]). Importantly, even under repeated analysis ($N = 20$) with the highest concentration standard (*i.e.*, 21.6 ppm), the device fully recovers its baseline and exhibits almost identical response of 0.160 ± 0.002, demonstrating the lack of carryover effect (*i.e.*, complete desorption, Fig. S5†). The lower responses detected here in comparison to Fig. 2f are likely due to different flow conditions on the flow-bench compared to the pump, and the room air environment in which the baseline resistance is lower (*i.e.*, 32 kΩ compared to 33 kΩ in synthetic air).
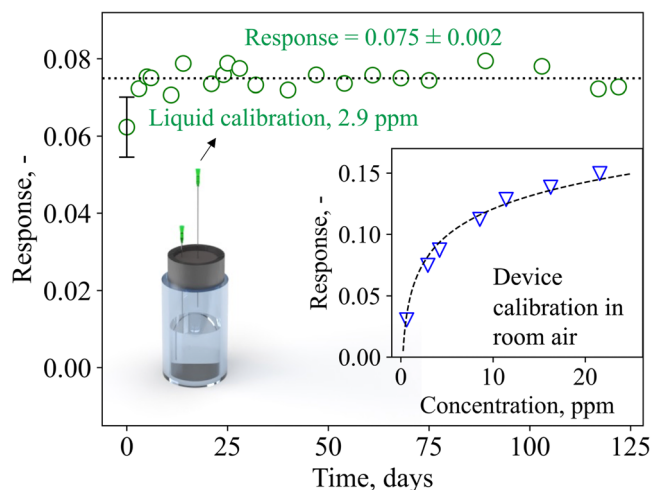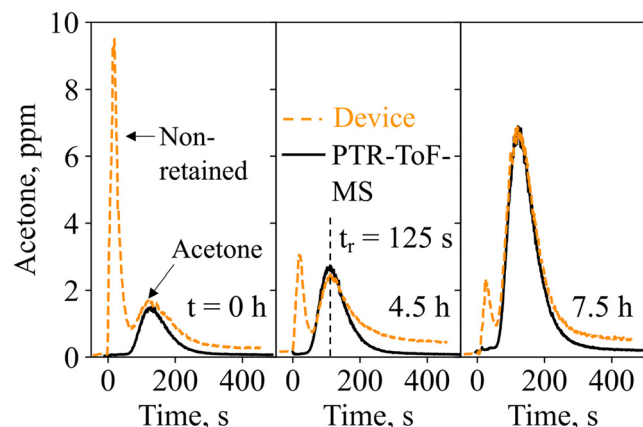
Fig. 4 Acetone concentrations as recorded by the device (dashed line) and PTR-ToF-MS (solid line) for three exhalations of volunteer #1 at t = 0 h (at 8:00), 4.5 h and 7.5 h of the ketogenic diet. The acetone retention time (t_r) is indicated with a dashed line.

3.3 Dynamic acetone monitoring in breath

Next, the device was tested on exhaled breath in real-life scenarios. End-tidal breath sampling with the tailor-made sampling unit was verified by monitoring the exhalations with a commercial CO_2 sensor (Fig. S6†). Within the

sampling unit, which was designed according to end-tidal breath samplers from the literature,[73] breath from the upper airways is separated from the end-tidal portion, which best reflects the blood chemistry and thus lipolysis.[74] This is confirmed by the final CO_2 concentrations of 6 ± 0.3% for three separately produced sampling units, being higher than 3%.[75]

Fig. 4 shows the quantified acetone concentrations as measured with the device and the PTR-ToF-MS for three breath exhalations of volunteer #1 at t = 0 h (8 am), 4.5 h, and 7.5 h of the ketogenic diet protocol. Notably, each breath exhalation is picked up by the device with an immediate sharp peak, followed by a second peak at 125 s, hence featuring similar response dynamics to the gas mixture measurements (Fig. 2e). The peak at 125 s corresponds to acetone, as validated by the PTR-ToF-MS, and increases over time (*i.e.*, from 1.6 to 6.8 ppm between 0 and 7.5 h), typical for ketogenic diet.[76] At the same time, almost no isoprene, ethanol, or methanol is detected at t = 125 s (Fig. S7†), as expected due to the catalytic filter and confirmed with PTR-ToF-MS. The slightly longer retention time of 125 s, compared to 100 s on the flow-bench, should be attributed to the difference in flow characteristics (Fig. S2†). It is worth noting that there is a large signal variation of the non-retained species between the three breath exhalations (*e.g.*,
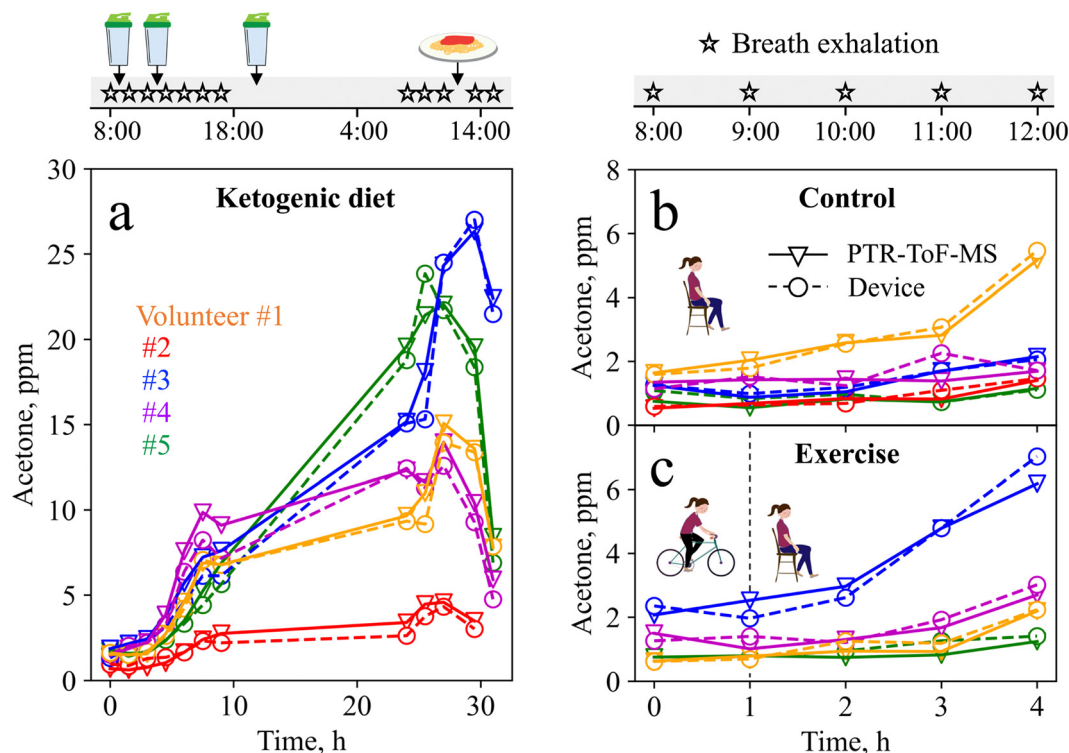

Fig. 5 Acetone concentrations quantified by the device (circles, dashed line) and PTR-ToF-MS (triangles, solid line) during a ketogenic diet (a), a control visit (b) and after an exercise stimulus (c) for volunteer #1 (orange), #2 (red), #3 (blue), #4 (purple), and #5 (green). The ketogenic diet protocol lasted for 31 h and ketogenic meals were consumed at t = 1, 4, and 11.5 h, while a carbohydrate rich pasta lunch was consumed the next day at t = 28 h. The control and exercise protocol lasted for 4 h, with a 45 min exercise stimulus (moderate cycling) during the first hour. Note that volunteer #2 did not give the last breath pulse of the ketogenic diet at t = 31 h due to a headache, and could not participate in the exercise protocol due to an injury.

quantified as 9.5, 3, and 2.2 ppm), highlighting again the importance of the catalytic filter and separation column (discussed in section 3.1), as otherwise, the acetone response would likely have been concealed by the interferents.

The complete ketogenic diet profiles for all volunteers are shown in Fig. 5a. Volunteer #1 shows a 4.25-fold increase in acetone during the first nine hours of a ketogenic diet, in line with the literature (*i.e.*, 3.5-fold increase during 12 h (ref. 76)), and reaches a maximum of 15 ppm the following day, indicating advanced ketosis. The intake of a carbohydrate-rich pasta meal after 28 h leads to a drop in acetone concentrations (down to 7.8 ppm after 31 h), resulting from a body fuel switch from fat (lipids) to sugars (glucose).[77] Similar profiles are observed for volunteers #2–5, all showing an increase in acetone concentration during the first 28 h of ketogenic diet, followed by a decrease after consumption of the pasta meal. Most importantly, good agreement is observed between the device and PTR-ToF-MS. Notably, the maximum acetone concentrations reached during the time of ketogenic diet vary significantly (*i.e.*, from 4.6 ppm for volunteer #2 to 24.6 ppm for volunteer #3), covering a wide range of concentrations, all being in the range of the liquid calibration (Fig. 3). The large inter-subject differences highlight again the need for personalized and longitudinal monitoring.

To challenge the device further, it was tested during a baseline and an exercise visit, as acetone concentrations here are typically lower, and higher resolution is required. Fig. 5b shows the device and PTR-ToF-MS-measured acetone concentrations during the baseline visit. For volunteers #2–5, acetone concentrations remain rather low (*i.e.*, between 0.5 and 2.1 ppm), as expected for this protocol.[12] Interestingly, volunteer #1 shows an unexpected 3-fold increase in acetone concentrations, which can probably be attributed to a carbohydrate-poor dinner consumed the evening before the measurement. Fig. 5c shows the measurement results from the exercise visit. Here, the increase in acetone concentrations is higher (3-fold on average) compared to the baseline visit, resulting from increased fat-burning after the exercise intervention, in line with the literature.[12] This is most pronounced for volunteer #3, who reaches a maximum acetone concentration of 7 ppm, indicating that the exercise protocol was highly effective to stimulate fat-burning.[12] Most importantly, the device tracks small acetone changes in good agreement with PTR-ToF-MS, and reflects inter- and intra-subject variations that arise from daily variations in nutrition and exercise.

3.4 Device bias and precision

To determine the device accuracy, the breath samples measured from all volunteers during the baseline, exercise, and ketogenic dieting visits were compared to PTR-ToF-MS. The total of 103 breath exhalations is presented in Fig. 6a. The device shows excellent agreement with the PTR-ToF-MS (R^2 = 0.988, r_p > 0.99), outperforming most state-of-the-art

acetone detectors that were tested on exhaled breath (*e.g.*, r_p = 0.95 with Ce–CuO,[29] r_p = 0.97 with Si/WO$_3$ (ref. 12)). In addition, it is capable of *quantifying* concentrations as low as 0.5 ppm and up to 26.3 ppm, while many commercial devices can only detect relative differences. Most importantly, the device measures acetone both at lower concentrations, as encountered during resting and exercise (*e.g.*, <5 ppm), and at higher concentrations, as found during ketogenic diet (*e.g.*, >20 ppm). Note that frequent use of the device with humid breath samples may lead to a faster deterioration of the separation column. This was however not observed for the same separation column used in this study on 103 breath exhalations.

For statistical analysis, we performed Bland–Altman analysis over the entire range of acetone concentrations detected. The analysis reveals heteroscedasticity in the measurement error, meaning increasing error with increasing acetone concentration (Fig. S8†). Hence, the mean difference and limits of agreement are also found to be a function of
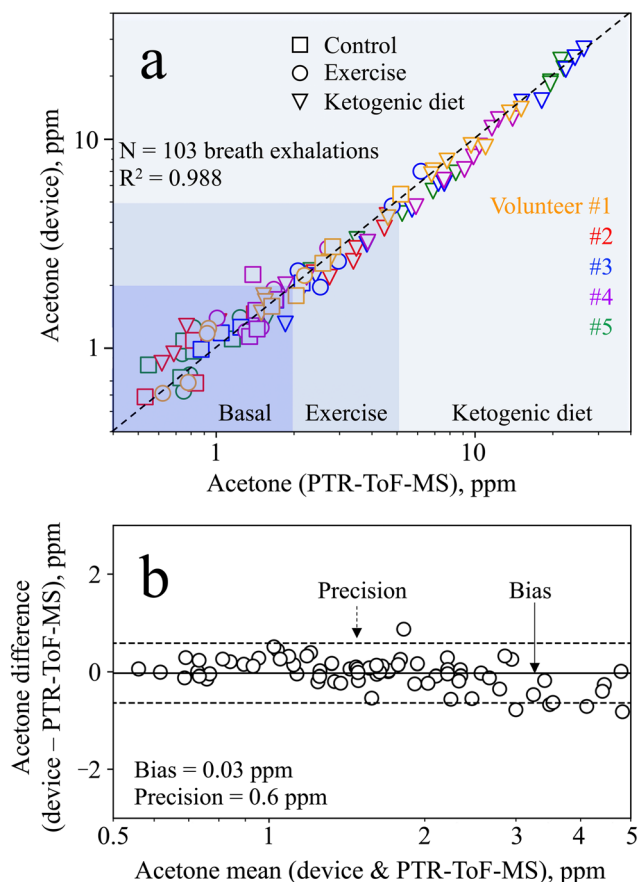

Fig. 6 (a) Scatter plot of N = 103 breath exhalations measured by the device and the PTR-ToF-MS for all five volunteers during the control (squares), the exercise (circles) and ketogenic diet (triangles) visit. Typical concentration ranges for basal acetone, after exercise, and during ketogenic diet are indicated. (b) Bland–Altman plot showing the difference in acetone concentration measured using the device and the PTR-ToF-MS as a function of the mean of both measurements for concentrations below 5 ppm. The bias and precision are indicated as solid and dashed lines, respectively.

the acetone concentration. This has been reported previously for similar sensors[78] and is partially attributed to the non-linear response behavior, saturating at higher concentrations (Fig. 3, inset, as discussed in section 3.1). For the purpose of tracking metabolic changes, the required precision strongly depends on the user case, and hence on the concentration range of interest. Specifically, this device features a relative bias and precision of 2% and 15%, respectively, at 10 ppm acetone (*i.e.*, an absolute precision of 1.5 ppm), making it well suitable to track ketogenic diets.

In the smaller concentration range, even better absolute precision is needed to track changes induced by exercise or other diets (*e.g.*, intermittent fasting). Therefore, Bland–Altman analysis is performed in the range between 0 and 5 ppm (Fig. 6b) to assess the device capability to distinguish between such small acetone concentrations. Most importantly, it features excellent bias and precision of 0.03 and 0.6 ppm, respectively, clearly outperforming medically certified commercial devices (*e.g.*, accuracy of 1 ppm with LEVL[79]). Hence, the device is capable of measuring exercise-induced changes, or even inter- and intra-subject changes during the baseline visit (Fig. 5b and c). It is worth noting that even better bias and precision may be achieved by equipping the device with a humidity and temperature sensor, to account for changes in retention time by the separation column.[39] In summary, however, the device shows excellent performance both in the lower concentration range (*e.g.*, to track exercise-induced lipolysis) and the higher concentration range (*e.g.*, to track ketogenic diets), making it highly attractive for a range of applications.

Conclusions

A handheld breath analysis device was presented with major benefits to monitor metabolic processes in individuals for predictive, personalized, participatory, and preventative point-of-care medicine. It featured compact size (6 × 10 × 19.5 cm^3), light weight (490 g), and simple operation through a touch-screen display. The device measured breath acetone and was equipped with a miniaturized breath sampler, a sensitive and selective acetone detector, a Raspberry Pi microcontroller, and a pump for on-demand breath sampling, all within a protective casing. The principle of selective acetone detection was the pre-screening of a sensitive but non-specific commercial sensor with a catalytic filter and a separation column, to remove or separate undesired interferents from acetone, hence enabling selective acetone within complex gas mixtures.

Device calibration was carried out through headspace sampling of portable liquid calibration standards, yielding a large dynamic acetone range (0.6–21.6 ppm) and excellent stability over at least four months. Importantly, individual device components, such as the catalytic filter, separation column, or sensor, could be readily replaced (plug-and-play), yielding comparable results (*i.e.*, deviations <15%). When tested on the exhaled breath of five volunteers, the device accurately tracked acetone concentrations during a ketogenic diet, a baseline visit, and before and after exercise. Most importantly, it featured excellent agreement with PTR-ToF-MS, and was capable of detecting the high concentrations observed during ketogenic diet (*e.g.*, >20 ppm), as well as resolving the small differences during the baseline visit or after exercise with a bias and precision of 0.03 and 0.6 ppm, respectively, for concentrations below 5 ppm, a task where commercial devices typically fail. This way, the device recognized the efficacy of the selected dieting and exercise stimuli for different volunteers, highlighting the need and potential of personalized monitoring.

Owing to its compactness, excellent stability, plug-and-play potential, and excellent bias and precision, this device could have significant implications for the management and treatment of metabolic diseases. We envision its use by doctors, patients, athletes, and individuals to guide lifestyle changes such as ketogenic diet, intermittent fasting, and exercising and improve personalized health care.

Author contributions

Grégoire Bastide: conceptualization, methodology, formal analysis, investigation, writing – original draft, writing – review & editing, visualization. *Anna Remund*: conceptualization, methodology, formal analysis, investigation, writing – original draft, writing – review & editing, visualization. *Dina Oosthuizen*: methodology, investigation, writing – review & editing, visualization. *Nina Derron*: methodology, investigation, writing – review & editing. *Philipp Gerber*: methodology, investigation, writing – review & editing, supervision, funding acquisition. *Ines Weber*: conceptualization, methodology, formal analysis, investigation, writing – review & editing, visualization, supervision, funding acquisition.

Conflicts of interest

There are no conflicts to declare.

Acknowledgements

References

1 J. Kim, R. Ghaffari and D. H. Kim, *Nat. Biomed. Eng.*, 2017, **1**, 1–4.

2 R. Horne, J. I. Bell, J. R. Montgomery, M. O. Ravn and J. E. Tooke, *Lancet*, 2015, **385**, 1153–1154.

3 J. Beauchamp, C. E. Davis and J. D. Pleil, *Breathborne Biomarkers and the Human Volatilome*, Elsevier, 2020.

4   B. Reddy, U. Hassan, C. Seymour, D. C. Angus, T. S. Isbell, K. White, W. Weir, L. Yeh, A. Vincent and R. Bashir, *Nat. Biomed. Eng.*, 2018, **2**, 640–648.

5   R. H. Eckel, K. G. M. M. Alberti, S. M. Grundy and P. Z. Zimmet, *Lancet*, 2010, **375**, 181–183.

6   WHO, WHO – obesity and overweight, https://www.who.int/news-room/fact-sheets/detail/obesity-and-overweight, (accessed 20 March 2023).

7   A. De Lorenzo, L. Romano, L. Di Renzo, N. Di Lorenzo, G. Cenname and P. Gualtieri, *Nutrition*, 2020, **71**, 110615.

8   M. Evans, K. E. Cogan and B. Egan, *J. Physiol.*, 2017, **595**, 2857–2871.

9   B. T. E. Andrews, W. Denzer, G. Hancock, A. D. Lunn, R. Peverall, G. A. D. Ritchie and K. Williams, *J. Breath Res.*, 2018, **12**, 036015.

10 K. Königstein, S. Abegg, A. N. Schorn, I. C. Weber, N. Derron, A. Krebs, P. A. Gerber, A. Schmidt-Trucksäss and A. T. Güntner, *J. Breath Res.*, 2021, **15**, 16006.

11 R. Schubert, H. Schwoebel, A. Mau-Moeller, M. Behrens, P. Fuchs, M. Sklorz, J. K. Schubert, S. Bruhn and W. Miekisch, *Metabolomics*, 2012, **8**, 1069–1080.

12 A. T. Güntner, N. A. Sievi, S. J. Theodore, T. Gulich, M. Kohler and S. E. Pratsinis, *Anal. Chem.*, 2017, **89**, 10578–10584.

13 S. Stekovic, S. J. Hofer, N. Tripolt, M. A. Aon, P. Royer, L. Pein, J. T. Stadler, T. Pendl, B. Prietl, J. Url, S. Schroeder, J. Tadic, T. Eisenberg, C. Magnes, M. Stumpe, E. Zuegner, N. Bordag, R. Riedl, A. Schmidt, E. Kolesnik, N. Verheyen, A. Springer, T. Madl, F. Sinner, R. de Cabo, G. Kroemer, B. Obermayer-Pietsch, J. Dengjel, H. Sourij, T. R. Pieber and F. Madeo, *Cell Metab.*, 2019, **30**, 462–476.e5.

14 A. T. Güntner, J. F. Kompalla, H. Landis, S. J. Theodore, B. Geidl, N. A. Sievi, M. Kohler, S. E. Pratsinis and P. A. Gerber, *Sensors*, 2018, **18**, 3655.

15 T. D. Swink, E. P. Vining and J. M. Freeman, *Adv. Pediatr.*, 1997, **44**, 297–329.

16 J. C. Newman, A. J. Covarrubias, M. Zhao, X. Yu, P. Gut, C. P. Ng, Y. Huang, S. Haldar and E. Verdin, *Cell Metab.*, 2017, **26**, 547–557.

17 J. W. Yoon and J.-H. Lee, *Lab Chip*, 2017, **17**, 3537–3557.

18 W. T. Koo, S. J. Kim, J. S. Jang, D. H. Kim and I. D. Kim, *Adv. Sci.*, 2019, **6**, 1900250.

19 I. C. Weber, P. Rüedi, P. Sot, A. T. Güntner and S. E. Pratsinis, *Adv. Sci.*, 2022, **9**, 2103853.

20 Z. El Khalidi, B. Hartiti, M. Siadat, E. Comini, H. M. M. M. Arachchige, S. Fadili and P. Thevenin, *J. Mater. Sci.: Mater. Electron.*, 2019, **30**, 7681–7690.

21 R. Yoo, A. T. Güntner, Y. Park, H. J. Rim, H. S. Lee and W. Lee, *Sens. Actuators, B*, 2019, **283**, 107–115.

22 M. I. Nemufulwi, H. C. Swart, K. Shingange and G. H. Mhlongo, *Sens. Actuators, B*, 2023, **377**, 133027.

23 A. Staerz, U. Weimar and N. Barsan, *Sensors*, 2016, **16**, 1815.

24 M. Epifani, E. Comini, R. Díaz, A. Genç, T. Andreu, P. Siciliano and J. R. Morante, *J. Alloys Compd.*, 2016, **665**, 345–351.

25 L. Wang, A. Teleki, S. E. Pratsinis and P. I. Gouma, *Chem. Mater.*, 2008, **20**, 4794–4796.

26 J. Shi, G. Hu, Y. Sun, M. Geng, J. Wu, Y. Liu, M. Ge, J. Tao, M. Cao and N. Dai, *Sens. Actuators, B*, 2011, **156**, 820–824.

27 Q. Q. Jia, H. M. Ji, D. H. Wang, X. Bai, X. H. Sun and Z. G. Jin, *J. Mater. Chem. A*, 2014, **2**, 13602–13611.

28 S. J. Choi, I. Lee, B. H. Jang, D. Y. Youn, W. H. Ryu, C. O. Park and I. D. Kim, *Anal. Chem.*, 2013, **85**, 1792–1796.

29 D. N. Oosthuizen and I. C. Weber, *Small Sci.*, 2023, 2200096.

30 A. Szkudlarek, K. Kollbek, S. Klejna and A. Rydosz, *Mater. Res. Express*, 2018, **5**, 126406.

31 S. J. Choi, B. H. Jang, S. J. Lee, B. K. Min, A. Rothschild and I. D. Kim, *ACS Appl. Mater. Interfaces*, 2014, **6**, 2588–2597.

32 M. Narjinary, P. Rana, A. Sen and M. Pal, *Mater. Des.*, 2017, **115**, 158–164.

33 S. Singkammo, A. Wisitsoraat, C. Sriprachuabwong, A. Tuantranont, S. Phanichphant and C. Liewhiran, *ACS Appl. Mater. Interfaces*, 2015, **7**, 3077–3092.

34 B. D. L. Costello, A. Amann, H. Al-Kateb, C. Flynn, W. Filipiak, T. Khalid, D. Osborne and N. M. Ratcliffe, *J. Breath Res.*, 2014, **8**, 14001.

35 D. J. Calloway, E. L. Murphy and D. Bauer, *Am. J. Dig. Dis.*, 1969, **14**, 811–815.

36 A. T. Güntner, S. Abegg, K. Königstein, P. A. Gerber, A. Schmidt-Trucksäss and S. E. Pratsinis, *ACS Sens.*, 2019, **4**, 268–280.

37 V. Ruzsányi and M. P. Kalapos, *J. Breath Res.*, 2017, **11**, 024002.

38 I. C. Weber, H. P. Braun, F. Krumeich, A. T. Güntner and S. E. Pratsinis, *Adv. Sci.*, 2020, **7**, 2001503.

39 J. Van den Broek, S. Abegg, S. E. Pratsinis and A. T. Güntner, *Nat. Commun.*, 2019, **10**, 4220.

40 I. C. Weber and A. T. Güntner, *Sens. Actuators, B*, 2022, **356**, 131346.

41 I. C. Weber, C. T. Wang and A. T. Güntner, *Materials*, 2021, **14**, 1839.

42 A. T. Güntner, M. Righettoni and S. E. Pratsinis, *Sens. Actuators, B*, 2016, **223**, 266–273.

43 V. Ruzsanyi, F. Lochmann, S. Jürschik, P. Mochalski, K. Unterkofler and C. A. Mayhew, *Origin and Emission of Volatile Biomarkers in Breath: End-tidal Perspective*, 2022.

44 D. P. Swain, K. S. Abernathy, C. S. Smith, S. J. Lee and S. A. Bunn, *Med. Sci. Sports Exercise*, 1996, **26**, 112–115.

45 A. T. Güntner, I. C. Weber, S. Schon, S. E. Pratsinis and P. A. Gerber, *Sens. Actuators, B*, 2022, **367**, 132182.

46 J. Freeman, P. Veggiotti, G. Lanzi, A. Tagliabue and E. Perucca, *Epilepsy Res.*, 2006, **68**, 145–180.

47 M. D. Mifflin, S. T. St Jeor, L. A. Hill, B. J. Scott, S. A. Daugherty and Y. O. Koh, *Am. J. Clin. Nutr.*, 1990, **51**, 241–247.

48 K. Schwarz, W. Filipiak and A. Amann, *J. Breath Res.*, 2009, **3**, 027002.

49 K. Schwarz, A. Pizzini, B. Arendacká, K. Zerlauth, W. Filipiak, A. Schmid, A. Dzien, S. Neuner, M. Lechleitner, S. Scholl-Bürgi, W. Miekisch, J. Schubert, K. Unterkofler, V. Witkovský, G. Gastl and A. Amann, *J. Breath Res.*, 2009, **3**, 27003.

50 A. Amann and D. Smith, *Volatile Biomarkers: Non-Invasive Diagnosis in Physiology and Medicine*, Elsevier, 2013.

51 M. Müller, T. Mikoviny, S. Feil, S. Haidacher, G. Hanel, E. Hartungen, A. Jordan, L. Märk, P. Mutschlechner, R. Schottkowsky, P. Sulzer, J. H. Crawford and A. Wisthaler, *Atmos. Meas. Tech.*, 2014, **7**, 3763–3772.

52 A. D. McNaught and A. Wilkinson, *IUPAC, Compendium of Chemical Terminology, (the 'Gold Book')*, Blackwell Scientific Publications, Oxford, 2nd edn, 1997.

53 C. J. Geankoplis, *Transport Processes and Separation Process Principles*, Prentice Hall, 4th edn, 2003.

54 M. J. Bland and D. G. Altman, *Lancet*, 1986, 307–310.

55 JCGM, BIPM, The international vocabulary of metrology—basic and general concepts and associated terms (VIM), 3rd edn, https://www.bipm.org/utils/common/documents/jcgm/JCGM_200_2012.pdf, (accessed 8 November 2020).

56 M. Thompson, *Anal. Methods*, 2012, **4**, 1598–1611.

57 J. M. Bland and D. G. Altman, *Br. J. Med.*, 1996, **312**, 1079.

58 C. Turner, P. Španěl and D. Smith, *Physiol. Meas.*, 2006, **27**, 637–648.

59 J. King, A. Kupferthaler, K. Unterkofler, H. Koc, S. Teschl, G. Teschl, W. Miekisch, J. Schubert, H. Hinterhuber and A. Amann, *J. Breath Res.*, 2009, **3**, 27006.

60 V. Bessonneau and O. Thomas, *Int. J. Environ. Res. Public Health*, 2012, **9**, 868–879.

61 N. Burgos, M. Paulis, M. M. Antxustegi and M. Montes, *Appl. Catal., B*, 2002, **38**, 251–258.

62 Scientific Instrument Services, Tenax® TA Breakthrough Volume Data, https://www.sisweb.com/index/referenc/tenaxta.htm.

63 A. T. Güntner, L. Magro, J. van den Broek and S. E. Pratsinis, *iScience*, 2021, **24**, 102050.

64 S. Abegg, L. Magro, J. van den Broek, S. E. Pratsinis and A. T. Güntner, *Nat. Food*, 2020, **1**, 351–354.

65 J. van den Broek, D. K. Cerrejon, S. E. Pratsinis and A. T. Güntner, *J. Hazard. Mater.*, 2020, **399**, 123052.

66 U. C. Ghoshal, *J. Neurogastroenterol. Motil.*, 2011, **17**, 312–317.

67 H. W. Cheu, D. R. Brown and M. I. Rowe, *Am. J. Dis. Child.*, 1989, **143**, 156–159.

68 J. W. Gardner, *Sens. Actuators, B*, 1990, **1**, 166–170.

69 M. Frankel, G. Bekö, M. Timm, S. Gustavsen, E. W. Hansen and A. M. Madsen, *Appl. Environ. Microbiol.*, 2012, **78**, 8289–8297.

70 L. Ferrus, H. Guenard, G. Vardon and P. Varene, *Respir. Physiol.*, 1980, **39**, 367–381.

71 I. C. Weber, N. Derron, K. Königstein, P. A. Gerber, A. T. Güntner and S. E. Pratsinis, *Small Sci.*, 2021, **1**, 2100004.

72 D. V. Del Orbe, H. J. Park, M. J. Kwack, H. K. Lee, D. Y. Kim, J. G. Lim, I. Park, M. Sohn, S. Lim and D. S. Lee, *Sens. Actuators, B*, 2022, **369**, 132192.

73 S. Schon, S. J. Theodore and A. T. Güntner, *Sens. Actuators, B*, 2018, **273**, 1780–1785.

74 J. Herbig, T. Titzmann, J. Beauchamp, I. Kohl and A. Hansel, *J. Breath Res.*, 2008, **2**, 037008.

75 F. Di Francesco, C. Loccioni, M. Fioravanti, A. Russo, G. Pioggia, M. Ferro, I. Roehrer, S. Tabucchi and M. Onor, *J. Breath Res.*, 2008, **2**, 037009.

76 K. Musa-Veloso, S. S. Likhodii and S. C. Cunnane, *Am. J. Clin. Nutr.*, 2002, **76**, 65–70.

77 D. Smith, P. Spanel and S. Davies, *J. Appl. Physiol.*, 1999, **87**, 1584–1588.

78 J. Van den Broek, D. Bischof, N. Derron, S. Abegg, P. A. Gerber, A. T. Güntner and S. E. Pratsinis, *Anal. Chem.*, 2021, **93**, 1170–1178.

79 LEVL, Instruction manual, https://levlcare.com/wp-content/uploads/2022/01/LEVL-Instruction-Manual_2151-1028735-Rev-M-1.11.22-4.pdf, (accessed 31 March 2023).